4

Chitin Nanofibers with a Uniform Width of 10 to 20 nm and Their Transparent Nanocomposite Films

Shinsuke Ifuku, Antonio Norio Nakagaito and Hiroyuki Saimoto
Graduate School of Engineering, Tottori University, Koyama-cho Minami, Tottori, Japan

1. Introduction

Nanofibers have been paid much attention in research community due to the recent developments in nanotechnology. Generally, nanotechnology deals with structures sized 1-100 nm in at least one dimension. Nanotechnology may create many new materials and devices with a vast range of applications such as in medicine, electronics, biomaterials and energy production. As described in some reports, the fabrication of nanofibers is the subject of much attention because of their unique characteristics such as a very large surface area to mass ratio and other properties, which allow many promising properties for advanced applications. Nanofibers have been produced by a variety of methods. Most nanofibers are artificially prepared by electrospinning process, which produces fibers from polymer solution using interactions between fluid dynamics, electrically charged surfaces and electrically charged liquids. However, the processability, biocompatibility, and biodegradability of the obtained composites are limited compared to those of natural polymers.

There is a growing interest in producing nanofibers from natural polymers, since they introduce additional functionalities such as biodegrability, biocompability, renewability and availability. A variety of nanofibers are produced in nature, such as collagen fibrils, fibroin in silk, deoxyribonucleic acid (DNA) with double helix, and so on.

Among the variety of nanofibers, cellulose microfibrils are the most abundant natural nanofiber in nature. Recently, Abe et al. succeeded in isolating cellulose nanofibers with a uniform width of approximately 15 nm from wood (Abe et al., 2007). Wood cell walls consist of stiff cellulose microfibrils, embedded in soft matrix substances such as hemicelluloses and lignin which behave just as adhesive between microfibrils. Due to the extended crystalline structure, the microfibrils have efficient physical properties; their Young's modulus is 138 GPa (Nishino et al., 1995), their tensile strength is at least 2 GPa, based on experimental results for kraft pulp, and their thermal-expansion coefficient in the axial direction is as small as 0.1 ppm/K (Nishino et al., 2004) . These structural features of wood cell walls make the wood stiff and tough, and are helpful in supporting the huge body of a tree. Since cellulose nanofibers are embedded in the matrix phase, they can be isolated by first removing the matrix and subsequently extracted as nanofibers by a very simple grinding treatment.

After cellulose, chitin is the second most abundant biomacromolecule in nature, existing mainly in exoskeletons of crabs, shrimps, and insects, and is synthesized in the amount 10^{10} to 10^{11} tons every year (Gopalan & Dufresne, 2003). Owing to its linear (1→4)-*β*-*N*-acetyl glycosaminoglycan structure with two reactive hydroxyl groups and an acetamide group per anhydro-*N*-acetylglucosamine unit, chitin has broad potential in the design of advanced polymeric biomaterials (Figure 1). However, most of chitin is discarded as industrial food residue without effective utilization. Thus, it is important to develop efficient use of chitin as a natural and eco-friendly material.

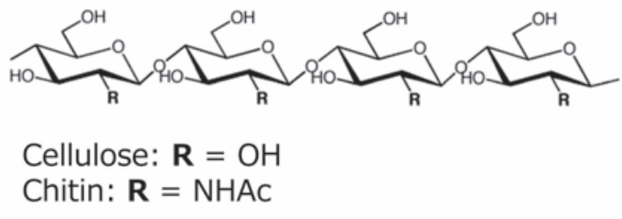

Fig. 1. Chemical structure of cellulose and chitin.

Native chitin in crab shells has highly crystalline structure, arranged as *α*-chitin in an antiparallel fashion forming microfibrils strongly connected by hydrogen bonds. The chitin microfibrils consist of nanofibers about 2–5 nm in diameter and about 300 nm in length embedded in several protein matrices (Raabe et al., 2006; Chen et al., 2008). Since chitin nanofibers are considered to have great potential, various methods have been employed for their preparation, such as acid hydrolysis (Gopalan & Dufresne, 2003; Revol & Marchessault, 1993), ultrasonication (Zhao et al., 2007), and electrospinning (Min et al., 2004). However, the nanofibers obtained by these processes were different from the native chitin nanofibers in terms of width, aspect ratio, crystallinity, chemical structure, and/or width distribution. Recently, Isogai et al, have developed an efficient method to prepare completely individualized cellulose nanofibers by 2,2,6,6-tetramethylpiperidine-1-oxy radical (TEMPO) mediated oxidation of native cellulose, followed by ultrasonic treatment. Although TEMPO mediated oxidation was applicable to crab shell *α*-chitin, the average nanocrystal length was considerably low (Fan et al., 2008a). In addition, the nanocrystals are actually chitin derivatives. They reported a procedure for preparing chitin nanofibers 3–4 nm in width from squid pen *β*-chitin by ultrasonication treatment under acidic conditions, however, the crystallinity of the nanofibers from the squid pen is relatively low (Fan et al., 2008b). Moreover, the biomass quantity of the pen is considerably lower than those of crab shells.

Similar to wood cell walls, the exoskeletons of crab and prawn have a strictly hierarchical structure consisting of crystalline *α*-chitin nanofibers and various types of proteins and minerals (mainly calcium carbonate) (Chen et al, 2008; Raabe et al, 2006; Giraud-guille, 1984). Thus, just like cellulose nanofibers, chitin nanofibers are embedded in matrix components. As Abe et al. described a preparation method can be used to isolate cellulose nanofibers from any natural plant containing lignin and hemicellulose, we considered that this isolation procedure would be applicable to any natural nanofiber source consisting of bionanofibers and other embedding matrixes. Accordingly, we here studied the extraction of natural *α*-chitin nanofibers with a uniform width of 10–20 nm from crab shells.

2. Preparation of chitin nanofibers

2.1 Chitin nanofibers from crab shell

In general, the crab shell has a strictly hierarchical organization which reveals various structural levels, as shown in Figure 2 (Chen et al., 2008; Giraud-guille, 1984; Raabe et al., 2005, 2006). Chitin molecules are aligned in an antiparallel manner that gives rise to α-chitin crystals in the form of thinner nanofibers. These nanofibers are wrapped in protein layers. The next level in the scale consists in the clustering of some of these nanofibers into chitin/protein fibers of about 50–300 nm in diameter. The next step is the formation of a planar woven and branched network of such chitin–protein fibers with a variety of thicknesses. These strands are embedded in a variety of proteins and minerals. The minerals mainly consist of crystalline calcium carbonate. The thickness of strands vary widely among crustaceans. Furthermore, these woven and networked planes form a twisted plywood pattern. This structure is formed by the helicoidal stacking sequences of the fibrous chitin-protein layers. The thickness of the twisted plywood layer corresponds to a certain stacking density of planes, which are gradually rotated about their normal axis.

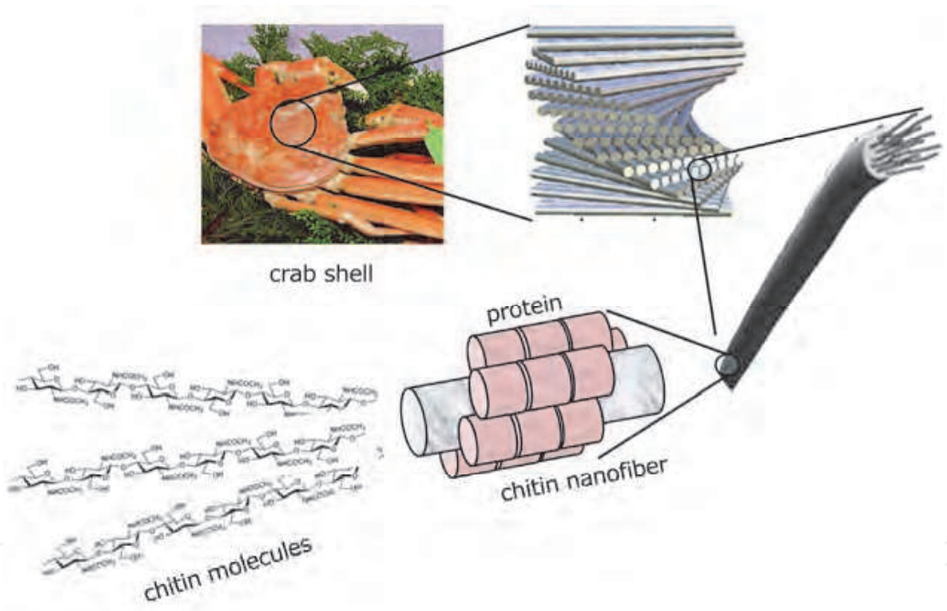

Fig. 2. Schematic presentation of the exoskeleton structure of crab shell.

To extract chitin nanofibers from crab shell, the samples were purified by a series of chemical treatments according to the flowchart shown in Figure 3. Dried crab shell flakes of *Paralithodes camtschaticus* (Red king crab), which is commercially available as a fertilizer at low cost were used for this study as the starting material. Crab shell powder was purified according to the general method. First, crab shell flakes were treated with 2 N HCl for 2 days at room temperature to remove the mineral salts. The suspension was filtered and washed thoroughly with distilled water. The sample was refluxed in 2 N NaOH for 2 days to remove the various proteins (Gopalan & Dufresne, 2003; BeMiller & Whistler, 1962, Shimahara & Takiguchi, 1998).

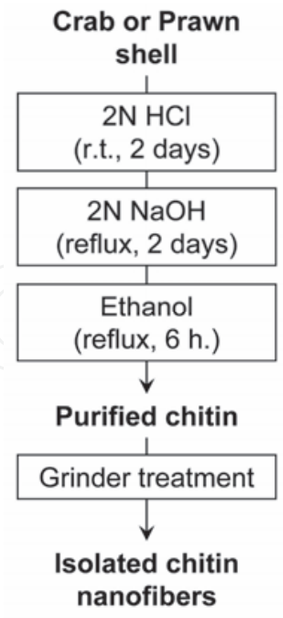

Fig. 3. Preparation procedure of chitin nanofibers from crab and prawn shell.

After filtration and rinsing with distilled water, the pigments and lipids in the sample were extracted by ethanol followed by filtration and rinsing with water (Shimahara & Takiguchi, 1998). It is known that almost all proteins and minerals (mainly calcium carbonate) can be removed by treatment with NaOH and HCl solutions each <0.1%. On the other hand, since complete removal of hemicelluloses from wood fiber is difficult, considerable amount of hemicelluloses remain in cellulose by alkali treatment. The yield of chitin from the crab shells was estimated to be 12.1 wt %. Since the process of drying chitin nanofibers generates strong hydrogen bonding between the nanofiber bundles, making difficult to obtain thin and uniform nanofibers, the material was kept wet after the removal of the matrix. Figure 4 shows field emission scanning electron microscope (FE-SEM) images of the crab shell surface after the removal of the matrix. The image represents the endocuticle, which makes up approximately 90 vol.% of the crab exoskeleton. We could observe that the chitin was made up of regularly structured chitin fiber networks, and the networks were found to be comprised of bundles of chitin nanofibers.

The purified wet chitin from dry crab shells was dispersed in distilled water at 1 wt %, and the slurry was passed through a grinder (MKCA6-3; Masuko Sangyo Co., Ltd.) under a neutral pH condition, with a careful adjustment of the clearance between the grinding stones. In principle, there is no direct contact between the grinding stones due to the presence of chitin suspension. The suspension of chitin fibrils was subjected to oven-drying after replacement of water by ethanol, and the obtained sheets were coated with an approximately 2 nm layer of platinum by an ion sputter coater and observed with FE-SEM. The widths of the fibers derived from crab shell after grinder treatment were widely distributed over a range 10 to 100 nm (Figure 5a). The chitin fiber network structure seems to have been broken completely by the grinder treatment after removal of the matrix substances. However the thicker fibrils of approximately 100 nm, which were bundles of nanofibers of 10–20 nm in width, still remained after grinder treatment even though the protein layers were removed under a never-dried condition.

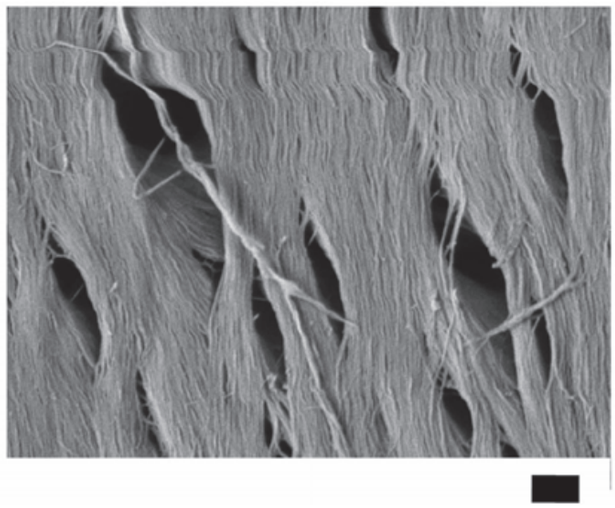

Fig. 4. FE-SEM image of crab shell surface after the removal of matrix. The length of scale bar is 300 nm.

Fan et al. reported a preparation method of chitin nanofibers from squid pen β-chitin in water at pH 3–4 (Fan et al., 2008a). Cationization of C2 amino groups in β-chitin under an acidic condition is important to maintain the stable dispersion state by electrostatic repulsions. Therefore, we considered that the purified α-chitin from crab shell would also be well dispersed under an acidic condition by the cationization of the amino groups on the fiber surface, which would facilitate fibrillation into 10-20 nm chitin nanofibers. Thus, the pH value of the purified chitin suspension was adjusted to approximately 3 by the addition of AcOH, and then the chitin was subjected to a grinder treatment. It should be emphasized that the chitin slurry thus obtained formed a gel after a single pass through the grinder, as the extremely large surface area leads to high dispersion property in water, suggesting that fibrillation was successfully accomplished, (Abe et al., 2007). Figure 5b and 5c show FE-SEM micrographs of the dried chitin gel. The isolated chitins were highly uniform nanofibers with a width of 10–20 nm, suggesting that the fibrillation process was facilitated in acidic solution as expected. Since broken fibers are not observed even over a wide observation area, the aspect ratios of the nanofibers are very high. These results indicate that chitin nanofibers were successfully isolated from crab shells without altering their natural shape. Thus, the never-dried process that has previously been used to extract the cellulose nanofibers from wood cell walls was here proven applicable for the preparation of 10-20 nm chitin nanofibers from crab shells by mechanical grinding at pH 3–4 condition.

2.2 Characterization of chitin nanofibers

The degree of *N*-acetylation of the obtained chitin nanofibers were calculated from the C and N contents from the elemental analysis data by using an elemental analyzer, and was found to be 95%. Thus, the degree of substitution of amino group was just 5%, indicating that deacetylation hardly occurred after the removal of proteins with 2N NaOH, and chitin nanofibers were obtained as natural fibers. Thus, even though the ratio of amino group was only 5%, cationization of amino groups facilitated the fibrillation of chitin fibers into nanofibers and maintained the stable dispersion state in the water by electrostatic repulsions between the chitin nanofibers with cationic surface charges.

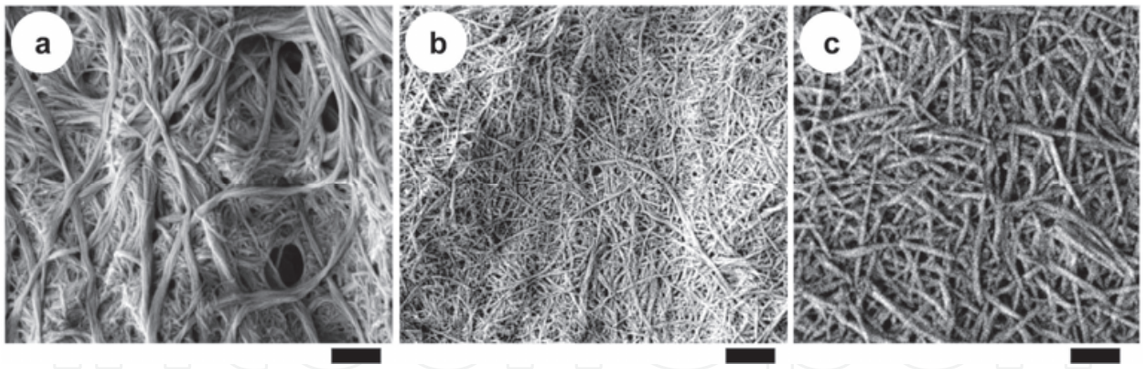

Fig. 5. SEM images of chitin nanofibers from crab shell after one pass through the grinder (a): under neutral pH condition, (b and c): under acidic condition at pH 3. The length of the scale bar is (a) 400 nm, (b) 400 nm, and (c) 200 nm, respectively.

Infrared spectra (FT-IR) recorded using potassium bromide pellets of (a) commercially available pure chitin, (b) newly prepared chitin nanofibers from crab shell, and (c) dried crab shell flakes without purification are shown in Figure 6. The spectrum of the dried crab shell flakes is very different from the other two spectra because of the matrix components included in the shell. On the other hand, the spectrum of newly prepared chitin nanofibers is in excellent agreement with the spectrum of commercial pure α-chitin, indicating that the matrix, protein and minerals were well removed by a series of processing steps. In particular, the absorption band at 1420 cm^{-1} derived from protein has completely disappeared, suggesting that these treatments were sufficient to eliminate all the proteins. Moreover, the OH stretching band at 3482 cm^{-1}, NH stretching band at 3270 cm^{-1}, amide I bands at 1661 and 1622 cm^{-1}, and amide II band at 1559 cm^{-1} of the chitin nanofibers are observed. These characteristic absorption peaks in the carbonyl region corresponds to anhydrous α-chitin (Gopalan & Dufresne, 2003).

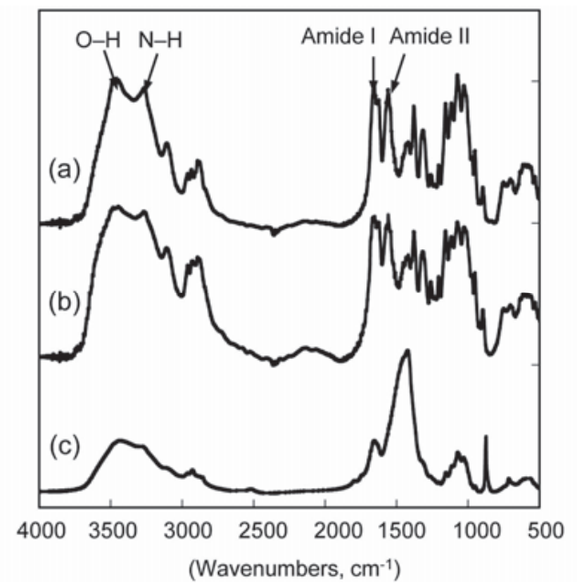

Fig. 6. FT–IR spectra of (a) commercially available chitin powder, (b) chitin nanofibers, and (c) crab shell flakes.

X-ray diffraction profiles obtained with Ni-filtered Cu Kα of (a) commercially available pure α-chitin, (b) newly prepared chitin nanofibers from crab shell, and (c) dried crab shell flakes derived from red king crab are shown in Figure 7. The diffraction peak at 29.6˚, which is typical of calcium carbonate, completely disappeared from the profile of chitin nanofibers, indicating that the mineral component was entirely removed from the newly prepared chitin nanofibers. The four diffraction peaks of chitin nanofibers observed at 9.5˚, 19.5˚, 20.9˚, and 23.4˚, which corresponds to 020, 110, 120, and 130 planes, respectively, are typical crystal patterns of α-chitin, and are closely coincident with commercial α-chitin (Minke & Blackwell, 1978). Thus, the chitin nanofibers were extracted from the crab shell, and the original molecular structure and α-chitin crystalline structure were maintained even after the removal of the matrix and the grinder treatments.

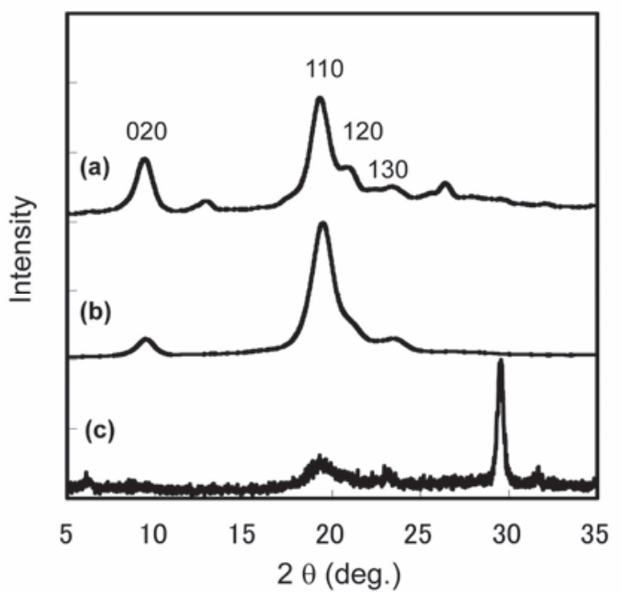

Fig. 7. X-ray diffraction profiles of a) commercially available chitin powder, (b) chitin nanofibers, and (c) crab shell flakes.

2.3 Chitin nanofibers from prawn shell

We succeeded in preparing α-chitin nanofibers from crab shells with a uniform width of approximately 10–20 nm (Ifuku et al., 2009). The grinder treatment under acidic conditions is the key to preparing chitin nanofibers. Cationization of amino groups in the chitin by the addition of an acid is important to maintain a stable dispersion state by electrostatic repulsions, which facilitate nano-fibrillation into chitin nanofibers. However, in some cases, the acidic condition may cause significant problems for application of chitin nanofibers such as in biomedical materials, nanocomposites, electronics devices, and so on, because in general, these materials are sensitive to acid. Indeed, it is difficult to remove acidic chemicals from chitin nanofiber suspension, since chitin nanofibers are homogeneously dispersed in water to give high viscosity. Therfore preparation of chitin nanofibers under a neutral pH condition is required to expand the application of nanofibers. Here, we show the extraction of chitin nanofibers from prawn shells under neutral conditions without using any acid.

Fresh shells of *Penaeus monodon* (black tiger prawn) was purified to prepare the chitin nanofibers. It is a widely cultured prawn species in the world and some of its shell is thrown away as industrial waste without effective utilization. Proteins and minerals were removed according to the conventional method using aqueous NaOH and HCl, respectively to extract the chitin component from the prawn shell (Shimahara & Takiguchi, 1998). The pigment component in the sample was then removed using ethanol. The yield of dry chitin from the wet prawn shells was approximately 16.7%. The degree of deacetylation (DDA) of the samples determined by the C and N content in the elemental analysis data was 7%. The SEM micrograph of the black tiger prawn shell surface after removal of the matrix components (without grinding treatment) is shown in Figure 8. This image is from the exocuticle, which is the main part of the prawn shell. Although the appearance of the prawn shell is still intact after removal of the matrix, we could observe uniform chitin nanofibers with an elaborate design.

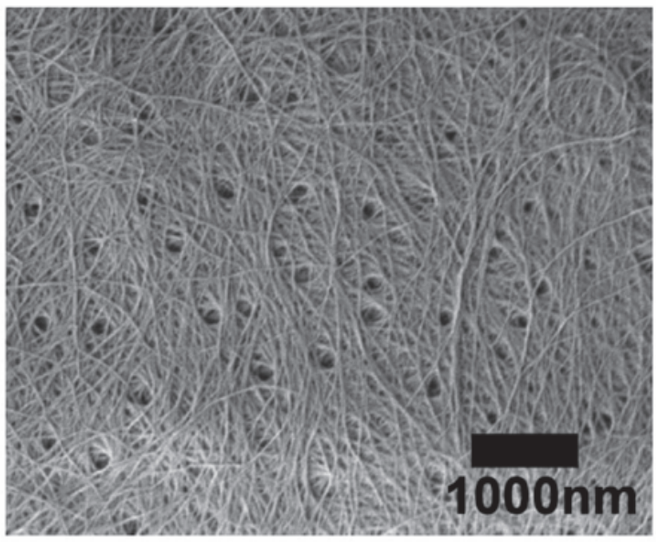

Fig. 8. FE-SEM image of the surface of the black tiger prawn after removing matrix components.

The purified chitin suspension with a concentration of 1 wt% was crushed by a domestic blender, and passed through a grinder for nano-fibrillation without using any acid. The chitin slurry thus obtained was viscous after a single grinding treatment similar to the chitin nanofibers from crab shell. The obtained chitin slurry was observed using FE-SEM (Fig. 9). In the case of crab shell, the widths of the fibers were widely distributed over a range from 10 to 100 nm by grinder treatment under a neutral condition as described above (Fig. 5a, Ifuku et al., 2009). On the other hand, in the case of prawn shell, we could see a uniform shape of chitin nanofibers using the same extraction treatment. The chitin nanofibers were highly uniform over an extensive area (Fig. 9a), and the width of the nanofibers was approximately 10 – 20 nm, including a 2 nm thick platinum coating layer (Fig. 9b). The fiber thickness of 10 – 20nm was similar to nanofibers from crab shell fibrillated under an acidic condition (Ifuku et al., 2009). Thus, chitin nanofibers were successfully prepared from prawn shell with a uniform width under a neutral pH condition.

The plausible explanation of successful fibrillation is following. The exoskeleton of crab and prawn is made up of mainly two parts, the exocuticle and the endocuticle. Although the exocuticle has a very fine twisted plywood-type structure, the endocuticle has a much coarser structure with a thicker fiber diameter (Fig. 4). In general, approximately 90% of a crab shell is made of endocuticle (Chen et al., 2008). In contrast, the exoskeleton of *Natantia*, which has a semitransparent soft shell, including the black tiger prawn, is made up primarily of a fine exocuticle, as shown in Figure 8 (Yano, 1972, 1975 & 1977). As a result, due to the differences in the cuticle structure, fibrillation of prawn shell is easier than that of crab shell.

The preparation method for chitin nanofibers from prawn shells under a neutral pH condition was applicable to other prawn shells. Figure 10 shows SEM images of the chitin nanofibers derived from (a) *Marsupenaeus japonicus* (Japanese tiger prawn) and (b) *Pandalus eous* (Alaskan pink shrimp), both of which are important food sources. These chitin nanofibers were prepared by the same preparation procedure, that is, removal of matrix components and subsequent grinding treatment under a neutral pH condition. Both chitins are also observed as uniform nanofibers with a width of 10–20 nm, which is similar to the nanofibers from black tiger prawn. This result suggests that chitin nanofibers can be obtained from other prawn species having a very fine exocuticle structure by nano-fibrillation under neutral pH conditions. Since many materials are sensitive to acid chemicals, this study will expand the application of chitin nanofibers.

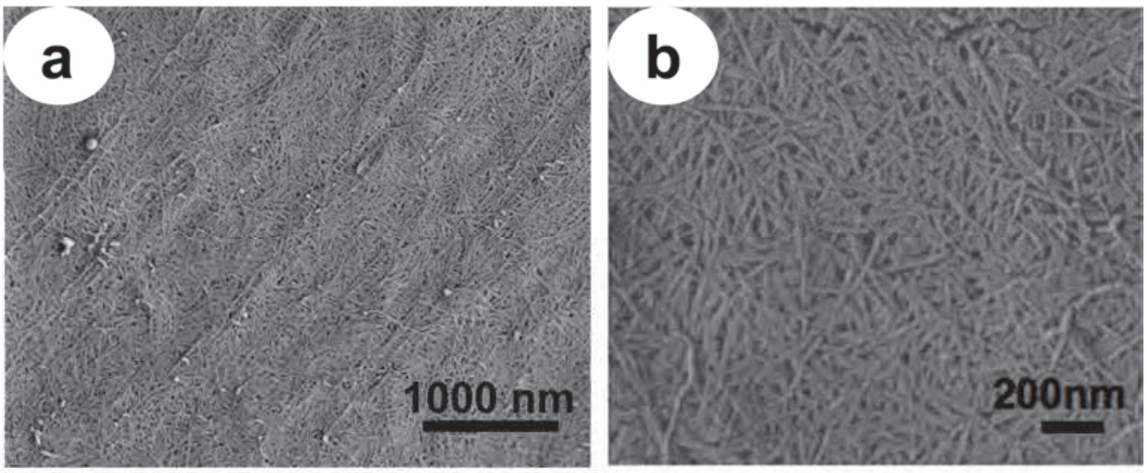

Fig. 9. FE-SEM images of chitin nanofibers from black tiger prawn shell after one pass through the grinder.

2.4 Facile preparation of chitin nanofiber from dry chitin

We have succeeded in isolating α-chitin nanofibers from crab and shrimp shells with a uniform width of 10–20 nm and a high aspect ratio (Ifuku et al., 2009). In general, the drying process of chitin and cellulose fibers generates strong hydrogen bonding between these fibers after removal of the matrix, which makes it difficult to fibrillate them into nanofibers. Therefore, chitin and cellulose must be kept wet after removal of the matrix for nanofiber preparation (Abe et al, 2007; Fan et al, 2009; Ifuku et al, 2009; Iwamoto et al., 2008; Saito et al., 2006). However, this requirement causes a strong disadvantage in the commercial

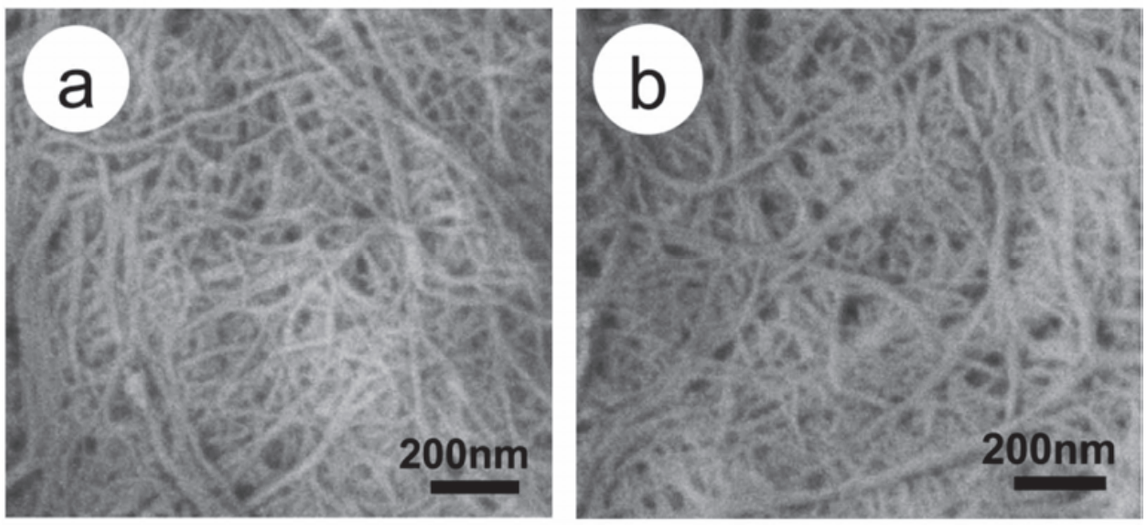

Fig. 10. FE-SEM images of chitin nanofibers (a) from Japanese tiger prawn shell, and (b) from Alaskan pink shrimp shell.

production of nanofibers. If chitin nanofibers could be obtained from dry chitin, we could prepare nanofibers easily and immediately whenever required. Therefore, preparation of nanofibers from a dried pure chitin is an important goal for expanding the use of chitin nanofiber. As described above, for the preparation of nanofibers, grinder treatment under an acidic condition is the key to fibrillating the chitin effectively (Fan et al., 2008b). A small number of amino groups in the chitin are cationized by the addition of an acid, which promotes the fibrillation of chitin into nanofibers by electrostatic repulsion. Indeed, electrostatic repulsion force is applied for the fibrillation of cellulose to obtain nanofibers through TEMPO-catalyzed oxidation too (Saito et al., 2006). If the electrostatic repulsion force of amino cations can break the strong hydrogen bonds between the chitin bundles, chitin nanofibers could be obtained from pure dry chitin aggregate. Accordingly, we here show the fibrillation of dried chitin into nanofibers by a grinding method under acidic conditions (Ifuku 2010b).

First, we tried to prepare cellulose nanofibers from dry pulp fibers, as a preliminary experiment. Figure 11 shows FE-SEM micrographs of cellulose fiber (a, b) before and (c) after single pass through the grinder with a concentration of 1 wt % for fibrillation of pulp fibers into cellulose nanofibers. In Figs. 11a and 11b, it can be seen that pulp fibers consist of a bundle of cellulose nanofibers. Figure 11c shows that the pulp fibers were not fibrillated into nanofibers at all after the grinder treatment. This is obviously because the drying process causes strong hydrogen bonding between the cellulose nanofibers after the removal of matrix substances hemicelluloses and lignin, thus making it difficult to obtain cellulose nanofibers. Thus, in general, the sample should never dry out for bionanofiber preparation after the removal of matrix (Abe et al., 2007; Iwamoto et al., 2008).

Next, we tried to fibrillate dried chitin into nanofibers. Dried chitin was prepared from crab shell flakes with an α-chitin crystal structure. The chitin was purified by the removal of matrix components of proteins and calcium carbonate according to the conventional method (Shimahara & Takiguchi, 1998), followed by drying in an oven to promote hydrogen bonding interaction between chitin nanofibers. Figure 4 is FE-SEM image of a crab shell after

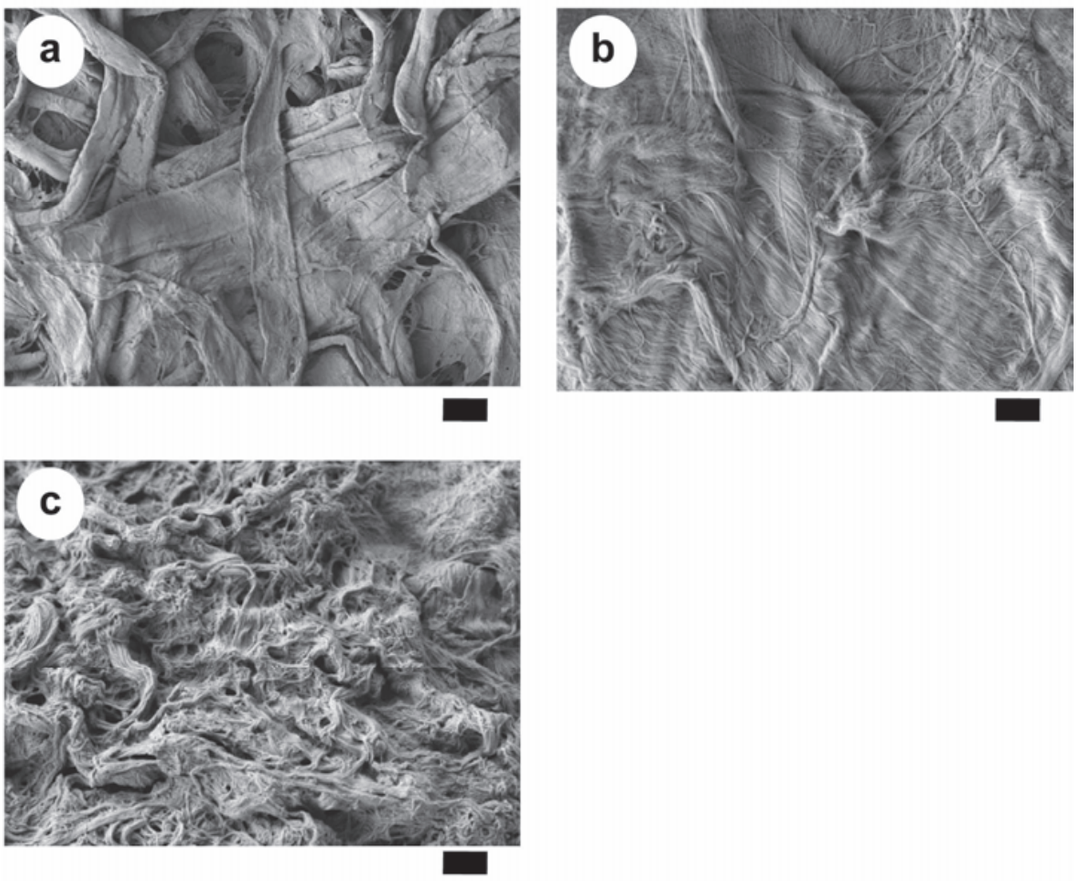

Fig. 11. FE-SEM images of cellulose fibers from wood pulp (a and b) before and (c) after one pass through grinder. The length of the scale bar is (a) 30,000 nm, and (b, c) 1000 nm, respectively.

removing matrices, followed by drying. It can be observed that the chitin was made up of structurally well organized bundles of nanofibers, as mentioned above. The slurry of purified dry chitin was passed through a grinder with a concentration of 1 wt % with and without acetic acid to fibrillate the bundles of chitin nanofibers. In the case of treatment under an acidic condition, the obtained chitin slurry had high viscosity, similar to the chitin nanofibers prepared by the previous method, suggesting that dried chitin was successfully fibrillated and homogeneously dispersed in acidic water with a very high surface ratio (Ifuku et al., 2009). Figure 12 shows FE-SEM images of chitin fibers after one pass through the grinder treated (a) without and (b, c) with acetic acid. In the case of grinder treatment under neutral pH condition, dried chitin could not be fibrillated at all, and aggregates of chitin nanofibers were observed (Fig. 12a). This lack of fibrillation also occurred because the drying process of purified chitin causes strong hydrogen bonding between hydroxyl, acetamide, and amino groups with strong dipole moments on the chitin fiber surface, which make it hard to fibrillate bundles of chitin nanofibers, as in the case of dry pulp fibers. On the other hand, chitin slurry treated at pH 3 was completely fibrillated into nanofibers (Fig. 12b and c).

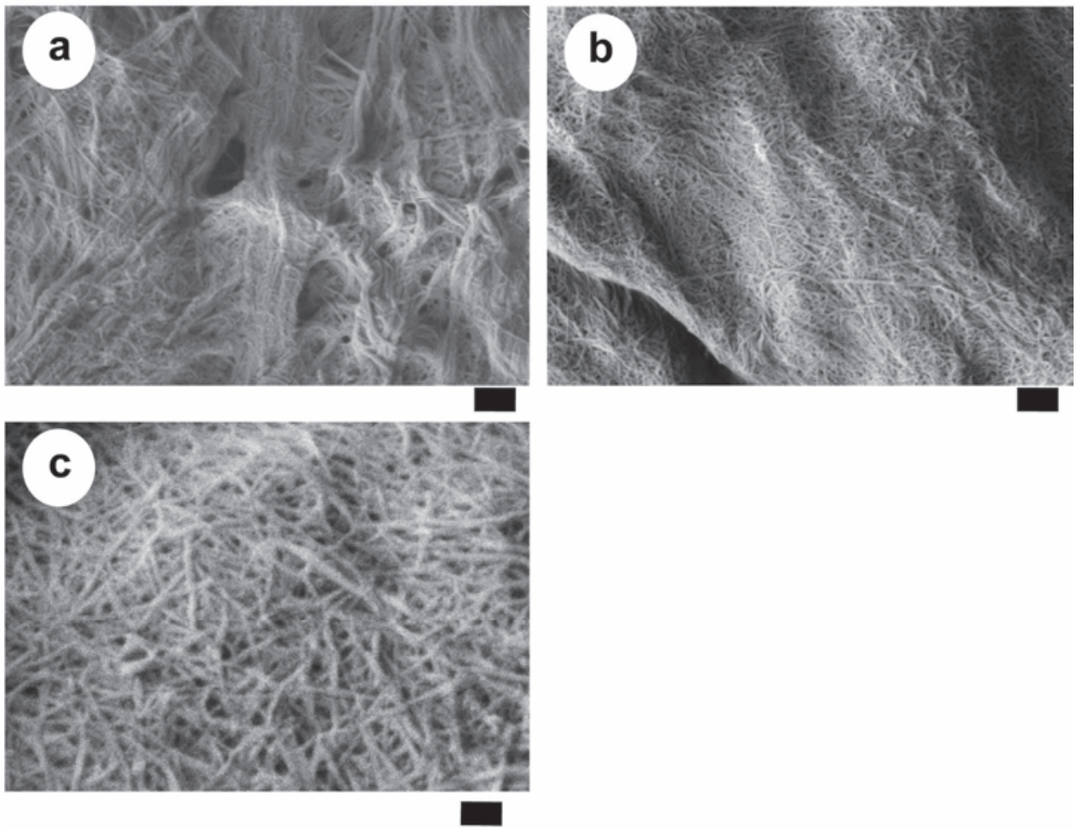

Fig. 12. FE-SEM images of chitin fibers after one pass through the grinder treated (a) without and (b, c) with acetic acid. The length of the scale bar is (a, b) 300 nm, and (c) 100 nm respectively.

The fibrillated chitin has a very fine nanofiber network; the structure is highly uniform with a width of 10 to 20 nm and a high aspect ratio, and we cannot see thicker fibers within the extensive area. The appearance of the fibers was very similar to nanofibers prepared with the never-dry process (Figs. 5b and c). The success of this new method is obviously owing to the electrostatic repulsions between the nanofibers. A few C2 amino groups on the chitin fiber surface were cationized under acidic conditions, which facilitated the fibrillation into nanofibers by electrostatic repulsions. Even though the degree of substitution of the amino groups calculated from the elemental analysis data was only 3.9 %, the electrostatic repulsion force caused from the cationic surface charges was enough to break the strong hydrogen bonds between the nanofibers. Thus, grinder treatment under acidic condition allowed us to obtain chitin nanofibers with a uniform width of 10–20 nm from purified dry chitin easily and immediately. This method could provide a significant advantage for industrial production of nanofibers from the viewpoints of stable supply, storage stability, transportation costs, storage space, and so on, since chitin nanofibers can be prepared by a simple method from light, low-volume, and nonperishable dried chitin. Use of the chitin nanofibers could be quite different from that of cellulose, which does not have ionic functional group to cause electrostatic repulsions. Since other acidic chemicals are also available to facilitate fibrillation, including ascorbic acid, lactic acid, citric acid, and so forth, several acidic additives are available for number of application.

The preparation method for chitin nanofibers was also found to be applicable to dry chitin powder purchased from a chemical reagent company. In Figure 13a, we can see well that commercially available dry chitin powder from crab shell is also made up of nanofibers (Chen et al., 2008; Raabe et al., 2005). Figure 13 shows FE-SEM micrographs of chitin fibers after one pass through the grinder (b) without and (c) with acetic acid, respectively. In Figure 13b, it can be seen that the chitin powder was not fibrillated at all because of the strong interfibrillar hydrogen bonding. On the other hand, in Figure 13c, the aggregates have clearly been fibrillated into homogeneous nanofibers with a width of 10 to 20 nm by grinder treatment at pH 3, even though the degree of substitution (DS) of amino groups was only 3.9 % and the slurry formed a gel. This is also owing to the electrostatic repulsion caused by cationic charges on the chitin fiber surface. In this way, since commercially available dry chitin powder is also made up of bundles of nanofibers, chitin nanofibers could easily be prepared from the dry chitin powder by applying electrostatic repulsion to break hydrogen bonds between chitin fibers' bundles. Chitin nanofibers from commercial prepurified dry chitin is advantageous for laboratory-scale investigations and commercial production because a large amount of chitin could be easily obtained within few hours by a simple fibrillation process under acidic conditions without any purification processes (removal of proteins, minerals, lipids, and pigments), which generally require at least 5 days (Shimahara & Takiguchi, 1998).

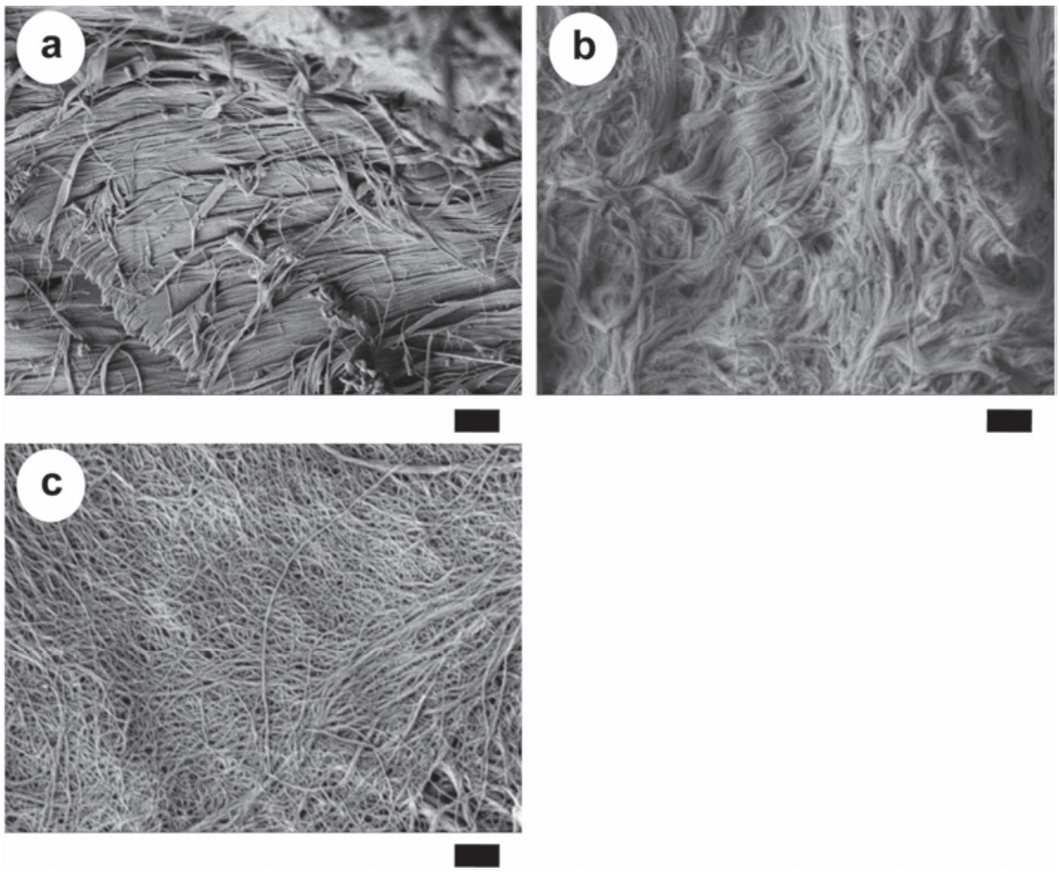

Fig. 13. FE-SEM images of (a) commercially available dry chitin powder, and chitin fibers after one pass through the grinder (b) without and (c) with acetic acid. The length of the scale bar is (a) 1000 nm and (b and c) 300 nm, respectively.

3. Preparation of optically transparent nanocomposites

3.1 Chitin nanofiber/acrylic resin composites

Since the chitin nanofiber consists of an antiparallel extended crystalline structure, the nanofiber has excellent mechanical properties: high Young's modulus and fracture strength, and low thermal expansion (Vincent & Wegst, 2004; Wada & Saito, 2001). Given the characteristic nano-form and efficient physical properties, the chitin nanofibers could be strong candidates for a reinforcement agent to create high-performance nanocomposites.

Ahead of the chitin nanofibers, cellulose nanofibers have attracted much attention in recent years as a reinforcement agent to make high performance nanocomposite (Nakagaito & Yano, 2008; Nakagaito et al., 2009). In particular, Yano et al. have fabricated a unique cellulose nanofiber composite film (Yano et al., 2005). Due to the nano-size effect, the nanocomposite film was optically transparent. This finding is applicable for chitin nanofibers to obtain optically transparent nanocomposite with acrylic resin as well (Ifuku, et al., 2010; Shams et al., 2011). We expect that the transparent chitin nanofiber/acrylic nanocomposite with improved mechanical and optical properties encourages the development of an optical device such as a flexible display. Additionally, chitin has different characteristics from cellulose such as biocompatibility (Tokura et al., 1983), wound healing activity (Okamoto et al., 1995), high purity (Shimahara & Takiguchi, 1998), and hydrophobicity (Shams et al., 2011), which strongly distinguish it from cellulose nanofiber reinforced composite film. In this study, we prepared chitin nanofiber composite with two different types of acrylic resins, and characterized their transparency, Young's modulus, mechanical strength, and thermal expansion. Specific characterization of the effects of chitin nanofibers on a variety of resins would be especially valuable for designing advanced nanocomposite materials.

Chitin nanofibers were prepared from commercially available dry chitin powder by fibrillation using a grinding apparatus. The fibrillated chitin samples were found to have a fine nanofiber network. The structure was highly uniform with a width of 10-20 nm and a high aspect ratio. Fibrillated chitin nanofibers were dispersed in water at a fiber content of 0.1 wt%. The suspension was vacuum-filtrated using a hydrophilic polytetrafluoroethylene membrane filter. The obtained chitin nanofiber sheets were hot-pressed to obtain a dried sheet. The chitin nanofiber sheets were cut into 3 cm × 4 cm sheets with approximately 45 μm thickness and a weight of 40 mg. The sheets were impregnated with bi-functional acrylic resins with 2 wt% of 2-hydroxy-2-methylpropiophenone photoinitiator under reduced pressure for 24 hours. Poly(propylene glycol) diacrylate (A-600) and tricyclodecanedimethanol dimethacrylate (DCP) were used in this study as acrylic resins (Fig. 14). The resin-impregnated sheets were polymerized using UV curing equipment. The chitin nanofiber composite films thus obtained were approximately 60 μm thick, and the fiber contents were approximately 40%.

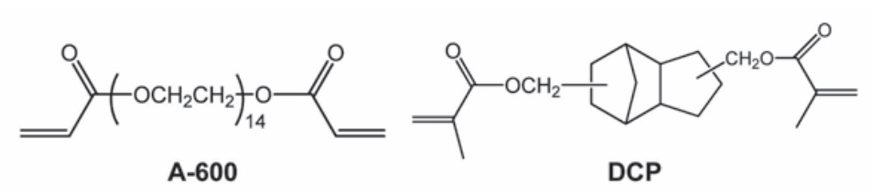

Fig. 14. Chemical structures of A-600 and DCP.

Both nanocomposite films were optically transparent despite the high fiber content of 40 wt%, due to the nanofiber size effect (Fig. 15, Yano et al., 2005). Figure 16 shows the regular light transmittance spectra of nanocomposites reinforced with chitin nanofibers. Transmittance of DCP nanocomposite was higher than that of A-600. This transparency is attributed to the difference in the refractive index (RI) of the resins. The RI of chitin nanofiber was reported to be 1.56 (Vigneron et al., 2005), which was closer to the RI of DCP than that of A-600, as shown in Table 1. The gap in the RI between chitin nanofiber and resins resulted in transparency difference.

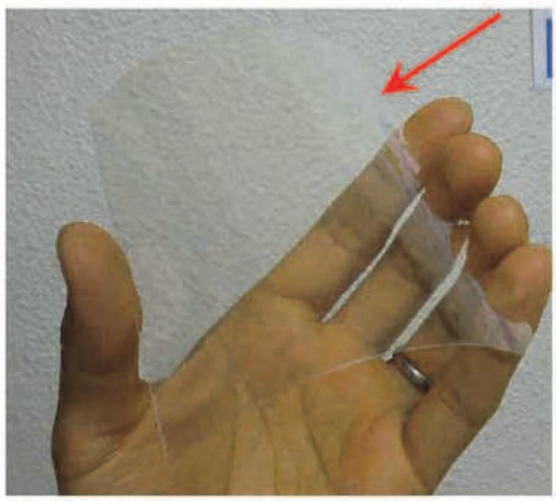

Fig. 15. Appearance of DCP films reinforced with chitin nanofibers.

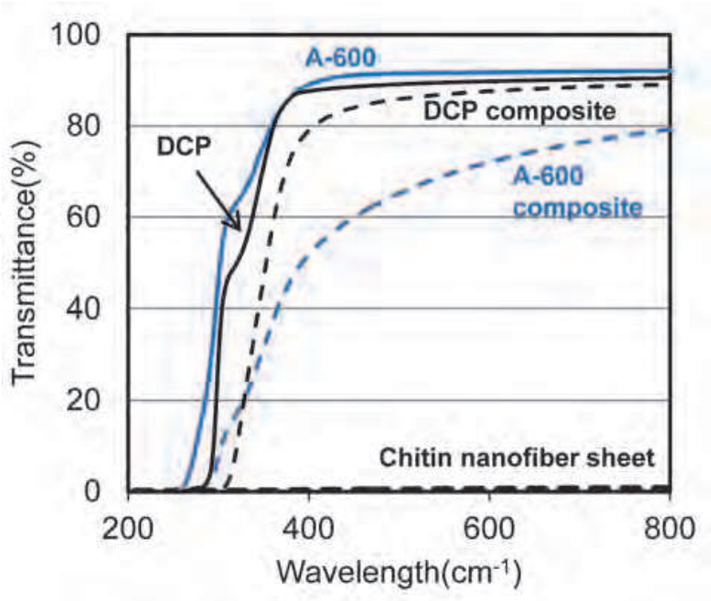

Fig. 16. Regular light transmittance spectra of neat acrylic resins (solid lines) and their nanocomposites (dashed lines).

	A-600		DCP		chitin nanofiber sheet
	neat resin	composite	neat resin	composite	
refractive index	1.468	-	1.500	-	-
transmittance (%)	91.8	72.1	89.8	87.6	0.4

Table 1. Regular light transmittance of neat acrylic resins and their nanocomposites at 600 nm.

Generally, thermal expansion has an inverse relationship with Young's modulus. Since the Young's modulus of chitin crystal is estimated to be at least 150 GPa (Vincent et al., 2005), the coefficient of thermal expansion (CTE) of chitin nanofiber sheet is only 10 ppm K^{-1}. Although the CTEs of A-600 and DCP were very high (184 and 100 ppm K^{-1}), the CTEs of their nanocompsites decreased drastically to 19 and 24 ppm K^{-1}, which corresponded to 90 and 76% decrease (Fig. 17 and Table 2). Thus, chitin nanofibers with low CTE and high Young's modulus could effectively decrease the CTE of acrylic resins by a reinforcement effect.

Since chitin nanofiber has high fracture stress and Young's modulus due to the antiparallel extended crystalline structure, it could be available as a reinforcing element to improve mechanical properties of a resin. The stress-strain curves of A-600 and DCP resin, and their nanocomposites are shown in Figure 18, and their mechanical properties are listed in Table 2. The Young's moduli of both resins effectively increased. Especially, Young's modulus of soft A-600 resin increased hundredfold, obviously due to the reinforcement with 40 wt% of chitin nanofiber. The tensile strengths of the two nanocomposites also successfully increased. These outstanding enhancements of mechanical properties strongly support the fact that chitin nanofiber with high Young's modulus and high tensile strength works effectively as a reinforcing element. Furthermore, chitin nanofiber can make a fragile resin ductile. That is, the DCP resin was extremely brittle due to its higher crosslinking density. However, the fracture strain of the DCP nanocomposite increased from 0.6 to 1.2%.

In conclusion, two types of acrylic resins reinforced with chitin nanofibers were highly transparent and flexible, and had low CTE, high Young's modulus, and high tensile strength, owing to the unique nano-size structure and excellent mechanical properties of chitin nanofiber.

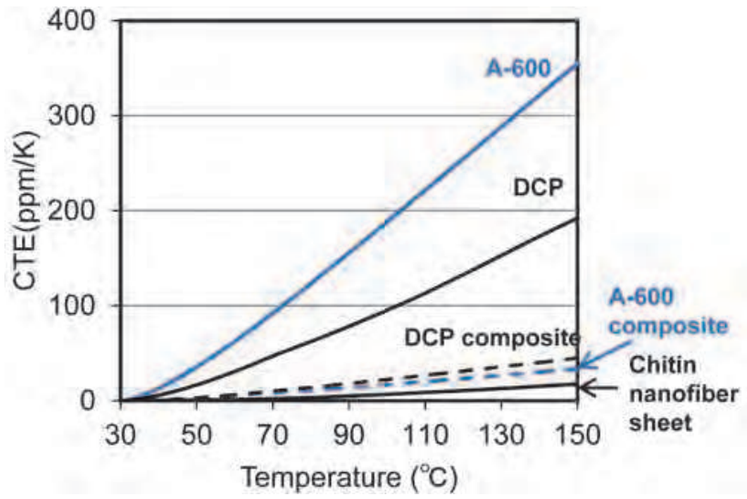

Fig. 17. Coefficients of thermal expansion of acrylic resins (solid lines) and their nanocomposites (dashed lines).

	A-600		DCP		chitin nanofiber sheet
	neat resin	composite	neat resin	composite	
Young's modulus (GPa)	0.02	2.03	2.30	5.34	2.50
fracture stress (MPa)	4	41	11	56	45
fracture strain (%)	16.5	9.0	0.6	1.2	7.8
CTE (ppm/K)	184	19	100	24	10

Table 2. Mechanical properties and CTEs of neat acrylic resins and their nanocomposites.

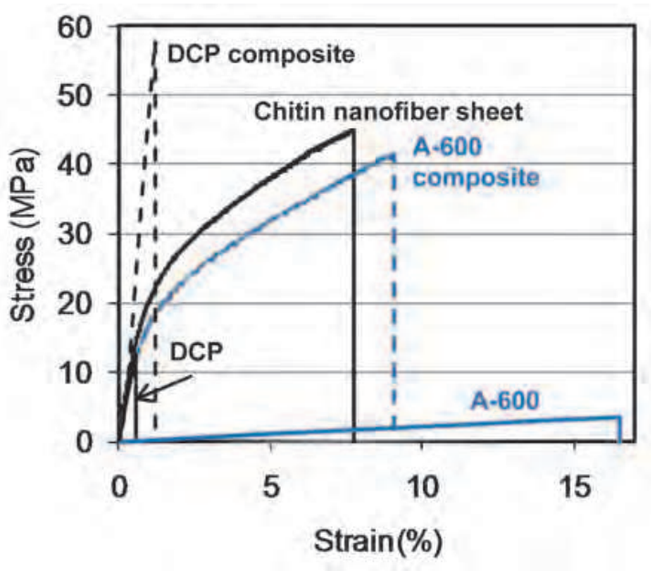

Fig. 18. Stress-strain curves of neat acrylic resins and their nanocomposites.

3.2 Acetylation of chitin nanofibers

We expect that chitin nanofibers with a uniform width and very high surface area will be developed into novel green nanomaterials. To expand the applications of chitin nanofibers, chemical modification of the chitin nanofiber surface is very important. By the introduction of hydrophobic functional groups into hydrophilic hydroxyl groups on chitin fibers, it is expected that dispersibility in nonpolar solvents, hygroscopicity, adhesion properties with hydrophobic matrices for fiber-reinforced composite materials are improved (Glasser et al., 1994). In chemical modification, acetylation is considered to be a simple, popular, and inexpensive approach to change the surface property (Kim et al., 2002; Ifuku et al., 2007). However, there have been no reports regarding acetylation of chitin nanofibers. Hence, the reaction behavior of highly crystalline chitin nanofibers, and the relationships between acetyl DS values and the various properties of the nanofibers remain unclear. We have showed that chitin nanofibers have very promising characteristics as a reinforcing material. The nanocomposites are optically transparent even with a high fiber content. We consider that acetylated chitin nanofiber would also be available as a filler to reinforce plastics. It is

therefore desirable to investigate acetyl DS dependency on the properties of chitin nanofiber composites, including transparency and hygroscopicity. We here prepared chitin nanofibers with different acetyl DS values and their nano-composites, and characterized them.
For acetylation of chitin nanofibers, the suspension of chitin nanofibers was vacuum-filtered using a membrane filter. The obtained chitin nanofiber sheets were dried and were cut into 3 × 4 cm sheets 60 μm thick, with a weight of 55 mg. The sheets were placed in a Petri dish containing a mixture of acetic anhydride and perchloric acid. The mixture was stirred for the desired time at room temperature. After acetylation, the chitin sheets were washed by Soxhlet extraction with methanol overnight Figure 19 shows the effects of reaction time on the DS of acetyl groups.

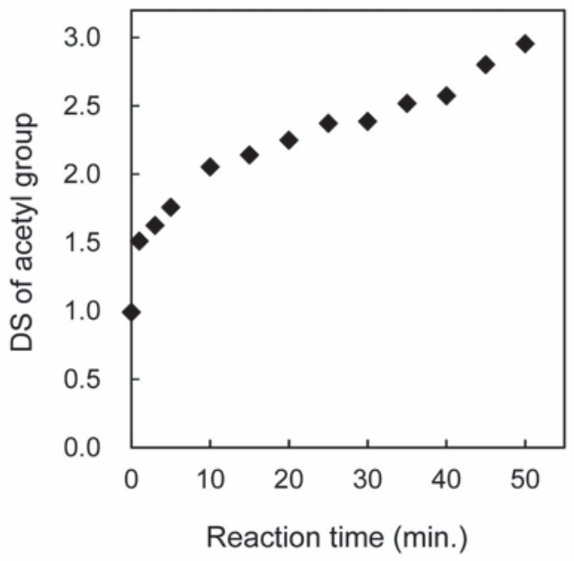

Fig. 19. Effect of reaction time on the acetyl DS.

The DS values were estimated by C and N content in the elemental analysis data. In general, since chitin has poor solubility in typical solvents, the reaction rate of acetylation of chitin is very small. However, in the case of chitin nanofibers, the acetyl DS ranged from 0.99 to 2.96 after 50 minutes reaction time, indicating an almost complete substitution of acetyl groups in the chitin nanofibers. The graph shows that the DS reached 1.51 from 0.99 after only 1 minute of acetylation. The high reaction rate is obviously due to the very high surface area, which works effectively for the liquid-solid phase reaction. The acetyl DS values then increased slowly and almost proportionally up to DS 2.96. The observed nonlinearity may have been caused by a heterogeneous reaction. That is, first, the chitin nanofiber surfaces were acetylated, and then the insides of the nanofibers were acetylated more gradually, as we describe later. Thus, the DS appears to be strictly adjustable by changing the acetylation time. This result could be applicable to other esterifications of chitin nanofibers using the corresponding acid anhydride.
The FT-IR spectra of acetylated chitin nanofibers with DS values of 0.99, 1.81, and 2.96 recorded using potassium bromide pellets are shown in Figure 20. As the DS of acetyl groups increased, two major bands at 1231 cm^{-1} and 1748 cm^{-1} increased, corresponding to the C-O and C=O stretching vibration modes of the acetyl group, respectively. In contrast,

the O-H stretching band at 3972 cm^{-1} decreased with increasing acetyl DS and almost disappeared with a DS of 2.96, indicating a complete substitution of acetyl groups in the chitin nanofibers.

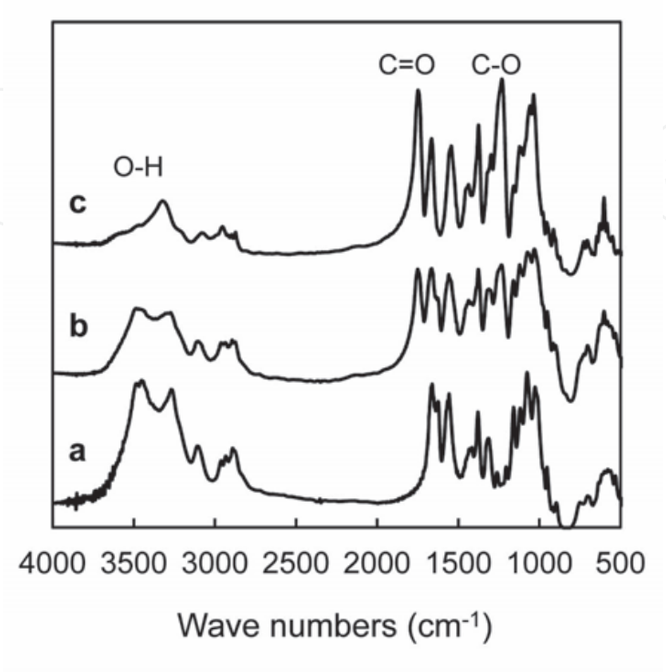

Fig. 20. FT-IR spectra of acetylated chitin nanofibers of (a) DS 0.99, (b) DS 1.81, and (c) DS 2.96.

Figure 21 shows the X-ray diffraction profiles of a series of acetylated chitin nanofibers. In original chitin nanofiber (DS 0.99), the four diffraction peaks of chitin nanofibers observed at 9.5, 19.4, 20.9, and 23.4°, which corresponds to 020, 110, 120, and 130 planes, respectively, show the typical antiparallel crystal pattern of α-chitin (Minke, 1978). At DS 2.96, the diffraction pattern from α-chitin had completely disappeared, and the sample showed a well-defined uniform pattern of di-*O*-acetylated chitin (chitin diacetate) at $2\theta = 7.4$ and 17.7°. On the other hand, the diffraction from α-chitin still remained even at DS 1.81, which indicates that approximately 50% of OH groups were substituted. Moreover, diffraction from chitin diacetate was also observed at 7.4°, and a small shoulder peak was also observed at 17.7°. This profile clearly shows that chitin nanofibers are acetylated heterogeneously from the surface to the core (Kim et al., 2002; Ifuku et al., 2007).

Figure 22 shows the FE-SEM images of acetylated chitin nanofibers with a series of DS values. Nanofiber shapes remain even in the DS 2.96 sample, which indicates that chitin diacetate is insoluble in the reaction mixture (mainly acetic anhydride), although cellulose triacetate is soluble in acetic anhydride. In all the images of the chitin nanofiber sheets, individual nanofibers seem to exist separately without aggregation, and as the DS values increase, the thickness of the nanofibers is increased. The average thicknesses of nanofibers with DS: 0.99, 1.81, and 2.96 were 21.6, 28.9, and 32.1 nm, respectively. This change in thickness is obviously due to the introduction of bulky acetyl groups into chitin nanofibers.

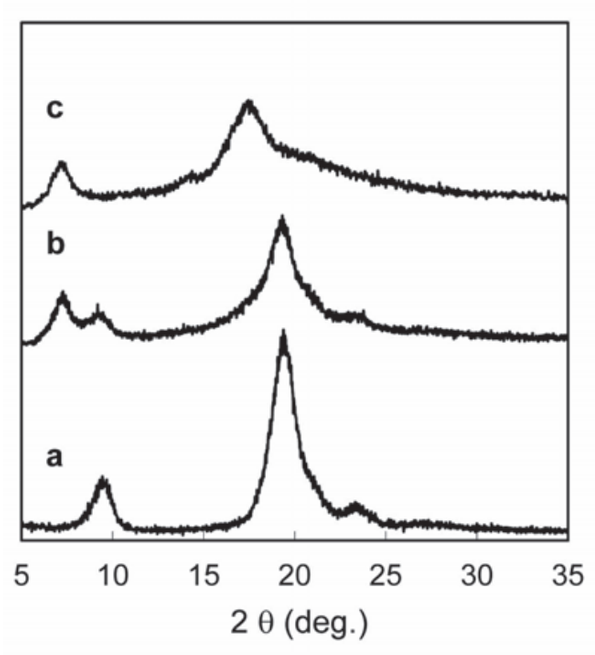

Fig. 21. X-ray diffraction profiles of acetylated chitin nanofibers of (a) DS 0.99, (b) DS 1.81, and (c) DS 2.96.

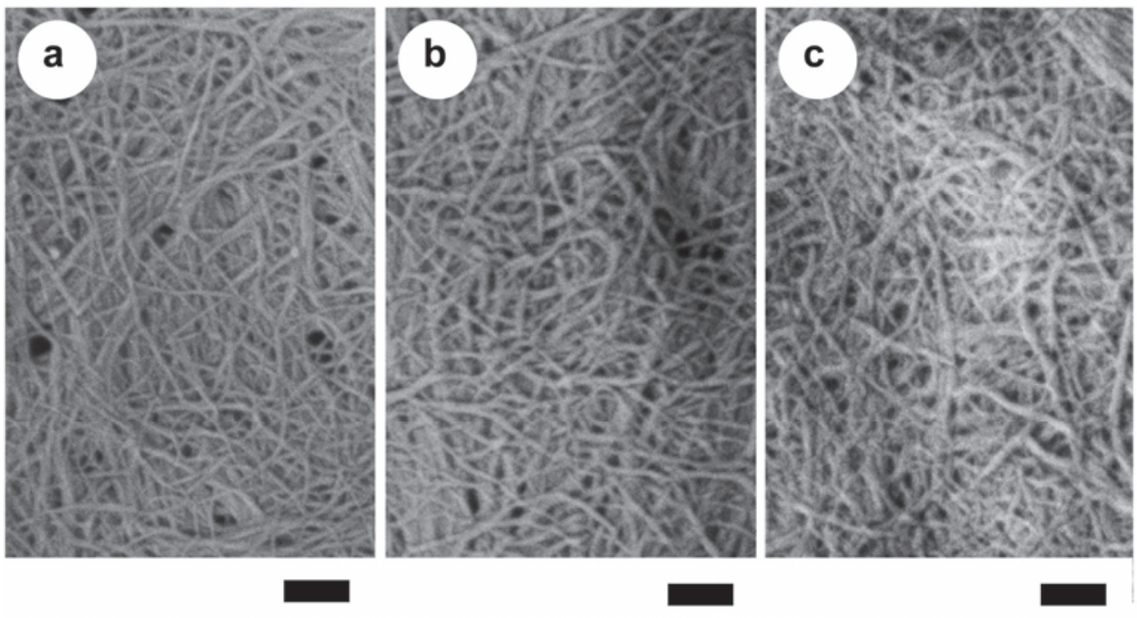

Fig. 22. FE-SEM micrographs of acetylated chitin nanofiber samples of (a) DS 0.99, (b) DS 1.81, and (c) DS 2.96 .The length of scale bar is 200 nm.

Thermogravimetric analysis (TGA) of a series of acetylated chitin nanofibers was carried out under nitrogen atmosphere to evaluate their degradation profiles and thermal stability. Figure 23 shows the derivative TGA curves of acetylated chitin nanofibers with DS 0.99, 1.81, and 2.96. The thermal degradation temperature of the original fibers (DS 0.99) was 388 ^{o}C according to the derivative curves. The derivative TGA curves drastically changed in the DS 2.96 sample, with no evidence of the peak derived from the original chitin nanofibers, and there were two peaks at 242 and 326 ^{o}C, which are attributed to the thermal decomposition of chitin diacetate. Interestingly, at DS 1.81, the TGA curve showed two kinds of thermal decomposition behaviors derived from chitin and chitin diacetate. This result obviously also indicates that acetyl groups were introduced from the surface to the core of the nanofibers.

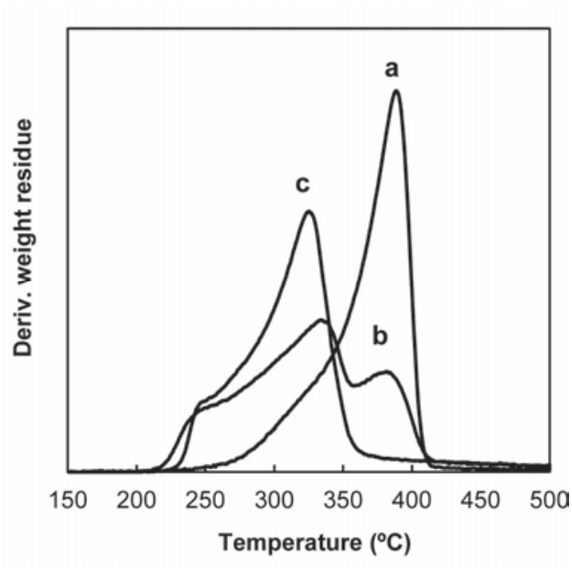

Fig. 23. Derivative TGA curves of acetylated chitin nanofibers of (a) DS 0.99, (b) DS 1.81, and (c) DS 2.96.

3.3 Characterization of acetylated chitin nanofiber composites

Acetylated chitin nanofiber composites were fabricated with acrylic resin DCP. The chitin nanofiber composite films thus obtained were approximately 150 μm thick, and the fiber content was approximately 25%. Since the diameters of the chitin nanofibers are sufficiently smaller than the visible light wavelength, all nanocomposites have high transparency despite a variety of acetyl DS values ranging from 0.99 to 2.96. Figure 24 shows the regular transmittance of a series of acetylated chitin nanofiber composites at 700 nm wavelength. At 0.99, the transparency of the nanocomposite was 77%. However, as the acetyl DS values increased, the transmittance decreased slightly and proportionally up to 73% at DS 2.96. This decrease can likely be attributed to the change in the refractive index of the nanofibers. The optimum refractive index of resin to obtain the highest transparency nanocomposite with chitin nanofibers is known to be approximately 1.56, which is close to that of the DCP resin (1.532, Vigneron, 2006). However, since acetylation decreases the refractive index, the gap in the refractive index between chitin nanofiber and resin became wider with acetylation, resulting in a reduction in transparency. The transparency of chitin nanofiber

composite was less sensitive to acetylation than that of bacterial cellulose (BC) nanofiber composite (Ifuku et al., 2006). The optical loss of the acetylated BC nanocomposite was approximately 20% with changes in the acetyl DS from 0.74 to 1.76. The difference of the optical loss is obviously due to the size effect. Since thickness of the chitin nanofiber is approximately 20 nm, which is considerably smaller than that of BC nanofibers (50 nm width), the chitin nanofibers are freer from light scattering than BC nanofibers (Nogi et al., 2005).

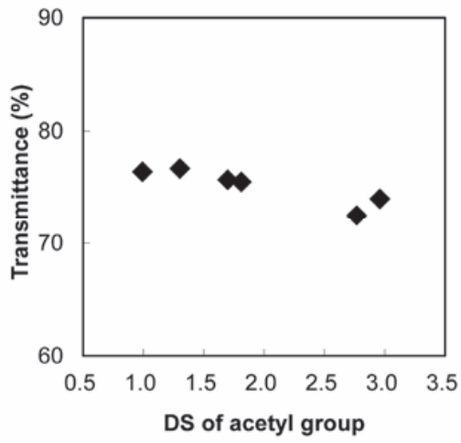

Fig. 24. Regular light transmittance of a series of acetylated chitin nanocomposites.

Although the chitin nanofiber reinforced composite seems to have promising characteristics as an optically functional composite, it is quite hygroscopic. Absorption of moisture causes deformation of the composite. Acetylation seems to reduce the moisture content of the nanocomposite. We therefore investigated the effects of acetylation on the hygroscopicity of the nanocomposites. Figure 25 shows the moisture content of a series of acetylated chitin nanofiber sheets and their composites. Moisture content was evaluated by exposing samples under a constant relative humidity. After measuring the sample weight equilibrated at 75.1% RH and 30 °C with a saturated aqueous solution of NaCl, the sample was oven-dried at 105 °C for 24 h, and the moisture content was then determined on the basis of the ovendried weight. Three samples were used to determine the moisture content. Interestingly, acetylation of chitin nanofiber sheet decreased its moisture content just slightly. The slight difference from 7.8% to 7.3% may be due to the nano-size effect. Since chitin nanofiber sheet with very high surface area was exposed to the air, water molecules were easily adsorbed onto the large nanofibers' surface. In the case of their composites, the moisture content of the original sample with DS 0.99 was 4.0%, which is considerably higher than the 0.33% of acrylic resin due to the hygroscopic chitin nanofiber filler. However, the moisture absorption of the nanocomposite with DS 1.30 drastically decreased to 2.2%. Clearly, this can be attributed to the introduction of hydrophobic acetyl groups into the hydrophilic hydroxyl moiety of chitin molecules. Acetylation of the nanofibers improved the compatibility with the acrylic resin, and improvement of miscibility at the filler/matrix interface decreased water adsorption onto the interface. However, with further acetylation, the moisture content showed little change, with a range of 2.0-2.5%. This result suggests that most hydroxyl groups on the chitin nanofiber surface were acetylated after 1 minute reaction time, as mentioned above.

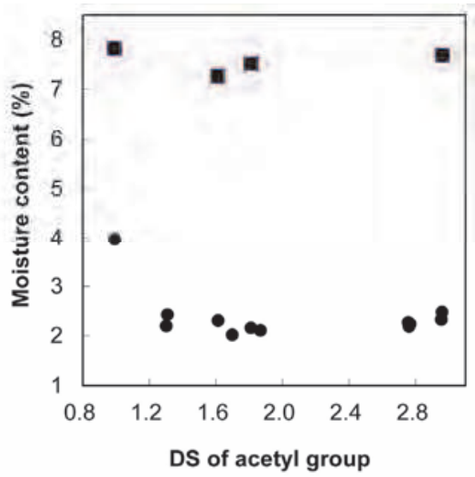

Fig. 25. Moisture contents of a series of acetylated chitin nanofiber sheets (squares) and their nanocomposites (circles).

Since chitin nanofibers have an extended antiparallel crystalline structure, the CTE of the nanofibers is small. We therefore thought that the chitin nanofibers act as a reinforcement agent to reduce the thermal expansion of a resin. However, the CTE of nanofibers and its composites will be changed by the acetylation. Figure 26 shows the CTE of chitin nanofiber sheets and DCP resin nanocomposites. The measurements were carried out from 30 to 165 °C by elevating the temperature at a rate of 5 °C min^{-1} in a nitrogen atmosphere in tensile mode. Although the CTE of the DCP resin was 64 ppm K^{-1}, the CTE of the chitin nanofiber/DCP composite was measured to be 23 ppm K^{-1}. It is easy to see that the chitin nanofibers with a low thermal expansion of 92 ppm K^{-1} drastically reduced the CTE of the DCP by reinforcement, with a fiber content of 25%. On the other hand, the CTE of chitin nanofiber samples and their composites increased proportionally and gradually with increases in the acetyl DS. This increase is due to the acetylation reducing the degree of crystallinity of the chitin nanofibers, as shown in Figure 21, which increases the CTE of chitin nanofibers and the nanocomposites.

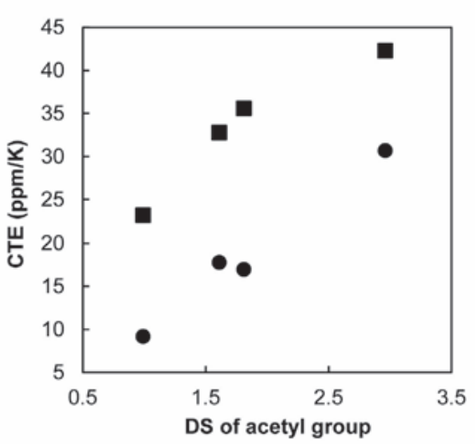

Fig. 26. Coefficient of thermal expansion of a series of acetylated chitin nanofibers (circles) and their nanocomposites (squares).

4. Conclusion

Chitin nanofibers were prepared from dried-crab shell which has a complex hierarchical structure with a uniform width of approximately 10-20 nm by conventional chemical treatment followed by mechanical treatment. This study demonstrates that the grinding treatment in a never-dried state after the removal of the matrix is applicable to not only wood but also crab shell to isolate nanofibers. Chitin nanofibers could be prepared from dried chitin as well. Mechanical treatment under acidic conditions is the key to fibrillating dried chitin. The cationization of amino groups on the chitin fiber surface breaks the strong hydrogen bonds between the nanofibers by electrostatic repulsion. These results indicate that the never-dried process is not necessary for chitin nanofiber preparation; this finding is quite different than that for cellulose nanofibers, since cellulose does not have ionic charges. Nanofibers from dry chitin are advantageous for commercial production in terms of storage, supply, transportation. This method allows us to effectively obtain homogeneous chitin nanofibers with a high surface-to-volume ratio. Moreover, chitin nanofibers could be prepared from a variety of prawn shells too. Since prawn shell has a finer structure than crab shell, chitin nanofibers were isolated without any acid.

Two different types of acrylic resins reinforced with chitin nanofibers were prepared. Due to nano-sized structure and excellent mechanical properties of chitin nanofiber, the composites were highly transparent and flexible, and had low thermal expansion, high Young's modulus, and high tensile strength. This study will expand the application of chitin nanofiber as a novel nanofiber reinforcement and encourage the use of chitin, most of which is thrown away as industrial waste, as a natural and environmentally friendly material.

Chitin nanofibers were chemically modified by acetyl groups. Acetylated chitin nanofibers with a variety of DS values were obtained by adjusting the reaction time. Acetyl groups were heterogeneously introduced inside the nanofibers after the surface reaction. X-ray diffraction profiles, SEM images, and TGA curves show that the acetylation of chitin nanofibers changes their crystal structure, fiber thickness, and thermal degradation temperature, respectively. Chitin nanofiber-reinforced plastics have high transparency with a variety of acetyl DS values. Acetylation reduced the moisture absorption of chitin nanocomposite by the introduction of hydrophobic acetyl groups.

As the thermal expansion is a property intrinsic to the material itself, its restriction depends on the reinforcing elements incorporated to the matrix. These reinforcements must not interfere with light transmittance in the case of transparent polymers. The use of natural nanofibers like chitin has proved to be a viable way to reduce the high thermal expansion of polymers without significant losses in transparency. These nanofibers are obtained from sustainable resources through environmentally friendly processes, and development of new extraction methods is attaining progressive cost reduction. As a result of this research, flexible transparent polymers with very low CTEs, low moisture adsorption, high Young's moduli, and high tensile strengths are emerging as potential candidates for optical functional devices.

5. References

Abe, K.; Iwamoto, S.; Yano, H. (2007). Obtaining cellulose nanofibers with a uniform width of 15 nm from wood. *Biomacromolecules*, 8: 3276 – 3278.

BeMiller, J. N.; Whistler, R. L. (1962). Alkaline Degradation of Amino Sugars. *J. Org. Chem.* 27: 1161 – 1164.

Chen, P.-Y.; Lin, Y.-M.; McKittrick, J.; Meyers, M. A. (2008). Structure and mechanical properties of crab exoskeletons. *Acta Biomateralia*, 4: 587 – 596.

Fan, Y.; Saito, T.; Isogai, A. (2008a). Chitin nanocrystals prepared by TEMPO mediated oxidation of α-chitin. *Biomacromolecules*, 9: 192 – 198.

Fan, Y.; Saito, T.; Isogai, A. (2008b). Preparation of chitin nanofibers from squid pen β-chitin by simple mechanical treatment under acid conditions. *Biomacromolecules*, 9: 1919 – 1923.

Fan, Y.; Saito, T.; Isogai, A. (2009). TEMPO-mediated oxidation of β-chitin to prepare individual nanofibrils. *Carbohydrate Polymers*, 77: 832 – 838.

Giraud-guille, M.-M. (1984). Fine structure of the chitin-protein system in the crab cuticle. *Tissue Cell,* 16: 75 – 92.

Glasser, W. G.; Taib, R.; Rajesh, R. K.; Kander, R. (1999), Fiber-reinforced cellulosic thermoplastic composites. *J. Appl. Polym. Sci.* 73: 1329 – 1340.

Gopalan Nair, K.; Dufresne, A. (2003) Crab shell chitin whisker reinforced natural rubber nanocomposites. 1. Processing and swelling behavior. *Biomacromolecules*, 4: 657 – 665.

Ifuku, S.; Nogi, M.; Abe, K.; Handa, K.; Nakatsubo, F.; Yano, H. (2007). Surface modification of bacterial cellulose nanofibers for property enhancement of optically transparent composites: Dependence on acetyl-group DS. *Biomacromolecules*, 8: 1973 – 1978.

Ifuku, S.; Nogi, M.; Abe, K.; Yoshioka, M.; Morimoto, M.; Saimoto, H., et al. (2009). Preparation of chitin nanofibers with a uniform width as α-chitin from crab shells. *Biomacromolecules*, 10: 1584 – 1588.

Ifuku, S.; Morooka, S.; Morimoto, M.; Saimoto, H. (2010a). Acetylation of chitin nanofibers and their transparent nanocomposite films. *Biomacromolecules*,11: 1326-1330.

Ifuku, S.; Nogi, M.; Yoshioka, M.; Morimoto, M.; Yano, H.; Saimoto, H. (2010b). Fibrillation of dried chitin into 10–20 nm nanofibers by a simple grinding method under acidic conditions. *Carbohydr. Polym.*, 81: 134-139.

Iwamoto, S.; Abe, K.; Yano, H. (2008). The effect of hemicelluloses on wood pulp nanofibrillation and nanofiber network characteristics. *Biomacromoles*, 9: 1022 – 1026.

Kim, D.-Y.; Nishiyama, Y.; Kuga, S. (2002). Surface acetylation of bacterial cellulose *Cellulose,* 9: 361 – 367.

Min, B. M.; Lee, S. W.; Lim, J. N.; You, Y.; Lee, T. S.; Kang, P. H.; Park, W. H. (2004). Chitin and chitosan nanofibers: Electrospinning of chitin and deacetylation of chitin nanofibers. *Polymer,* 45: 7137 – 7142.

Minke, R.; Blackwell, J. (1978). The structure of □-chitin. *J. Mol. Biol.,* 120: 167 – 181.

Nakagaito, A. N.; Yano, H. (2008). Toughness enhancement of cellulose nanocomposites by alkali treatment of the reinforcing cellulose nanofibers *Cellulose*, 15, 323-331.

Nakagaito, A. N.; Fujimura, A.; Sakai, T.; Hama, Y.; Yano, H. (2009). Production of microfibrillated cellulose (MFC)-reinforced polylactic acid (PLA) nanocomposites from sheets obtained by a papermaking-like process. *Compos. Sci. Technol.*, 69, 1293-1297.

Nishino, T.; Takano, K.; Nakamae, K. (1995). Elastic-modulus of the crystalline regions of cellulose polymorphs. *J. Polym. Sci., Part B: Polym. Phys.*, 33, 1647-1651.

Nishino, T.; Matsuda, I.; Hirano, K. (2004). All cellulose composite. *Macromolecules*, 37, 7683-7687.

Nogi, M.; Handa, K.; Nakagaito, A. N.; Yano, H. (2005). Optically transparent bionanofiber composites with low sensitivity to refractive index of the polymer matrix. *Applied Physics Letters*, 87: 243110.

Okamoto, Y.; Shibazaki, K.; Minami, S.; Matsuhashi, A.; Tanioka S.; Shigemasa, Y. (1995). Evaluation of Chitin and Chitosan on Open Wound Healing in Dogs. *J. Vet. Med. Sci*., 57, 851-854.

Raabe, D., Sachs, C., & Romano, P. (2005). The crustacean exoskeleton as an example of a structurally and mechanically graded biological nanocomposite material. *Acta Biomaterialia*, 53, 4281 – 4292.

Raabe, D.; Romano, P.; Sachs, C.; Fabritius, H.; Al-Sawalmih, A.; Yi, S. B.; Servos, G.; Hartwig, H. G., (2006). Microstructure and crystallographic texture of the chitin–protein network in the biological composite material of the exoskeleton of the lobster Homarus americanus. *Mater. Sci. Engin. A*., 421, 143-153.

Revol, J.-F., & Marchessault, R. H. (1993). In oifro chiral nematic ordering of chitin crystallites. International Journal of Biological Macromolecules, 15, 329 – 335.

Saito, T., Nishiyama, Y., Putaux, J.-L., Vignon, M., & Isogai, A. (2006). Homogeneous suspensions of individualized microfibrils from TEMPO-catalyzed oxidation of native cellulose. *Biomacromolecules*, 7, 1687 – 1691.

Shams, M. I.; Ifuku, S.; Nogi, M.; Oku, T.; Yano, H., (2011). Fabrication of optically transparent chitin nanocomposites. *Appl. Phys. A*, 102, 325-331.

Shimahara, K.; Takiguchi, Y. (1998). Preparation of crustacean chitin, In: *Methods in enzymology Vol. 161*, Wood, W. A.; Kellogg, S. T. (Eds.), pp. 417-423, Academia Press, 0121820629, CA.

Tokura S.; Nishi, N. Nishimura, S.; Somorin, O. (1983). Lysozyme-accessible fibers from chitin and its derivatives. *Sin-i Gakkaishi*. 39: 45-49.

Vincent, J.; Wegst, U. (2004). Design and mechanical properties of insect cuticle. *Arthropod Struct. Dev*., 33: 187-199.

Vigneron, J. P.; Rassart, M.; Vandenbem, C.; Lousse, V.; Deparis, O.; Biro, L. P.; Dedouaire, D.; Cornet, A.; Defrance, P. (2006). Spectral filtering of visible light by the cuticle of metallic woodboring beetles and microfabrication of a matching bioinspired material. *Phys. ReV. E*. 73: 041905.

Wada, M.; Saito, Y., (2001). Lateral Thermal Expansion of Chitin Crystals. *J. Polym. Sci. B*, 39: 168-174.

Yano, H., Sugiyama, J., Nakagaito, A. N., Nogi, M., Matsuura, T., Hikita, M., et al. (2005). Optically transparent composites reinforced with networks of bacterial nanofibers. *Advances Materials*, 17, 153 – 155.

Yano, I. (1972). A historical study on the exocuticle with respect to its calcification and associated epidermal cells in a shore crab. *Bull. of Jap. Soc. Sci. Fisheries,* 38: 733 – 739.

Yano, I. (1975). An electron microscope study on the calcification of the exoskeleton in a shore crab. *Bull. of Jap. Soc. Sci. Fisheries*, *Gakkaishi,* 41: 1079-1082.

Yano, I. (1977). Structures of exoskeletons of prawn and crab shells. *Kagaku to Seibutsu*, 15, 328 – 336.

Zhao, H.; Feng, X.; Gao, H. (2007). Ultrasonic technique for extracting nanofibers from nature materials. *Appl. Phys. Lett.* 90: 073112.

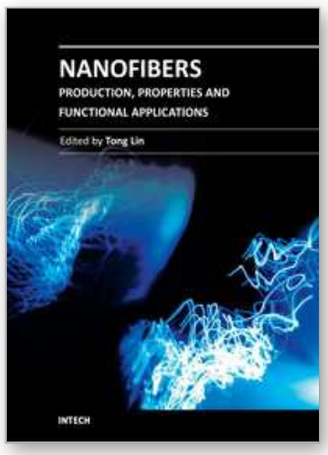

Nanofibers - Production, Properties and Functional Applications
Edited by Dr. Tong Lin

ISBN 978-953-307-420-7
Hard cover, 458 pages
Publisher InTech
Published online 14, November, 2011
Published in print edition November, 2011

As an important one-dimensional nanomaterial, nanofibers have extremely high specific surface area because of their small diameters, and nanofiber membranes are highly porous with excellent pore interconnectivity. These unique characteristics plus the functionalities from the materials themselves impart nanofibers with a number of novel properties for advanced applications. This book is a compilation of contributions made by experts who specialize in nanofibers. It provides an up-to-date coverage of in nanofiber preparation, properties and functional applications. I am deeply appreciative of all the authors and have no doubt that their contribution will be a useful resource for anyone associated with the discipline of nanofibers.

How to reference
In order to correctly reference this scholarly work, feel free to copy and paste the following:

Shinsuke Ifuku, Antonio Norio Nakagaito and Hiroyuki Saimoto (2011). Chitin Nanofibers with a Uniform Width of 10 to 20 nm and Their Transparent Nanocomposite Films, Nanofibers - Production, Properties and Functional Applications, Dr. Tong Lin (Ed.), ISBN: 978-953-307-420-7, InTech, Available from: http://www.intechopen.com/books/nanofibers-production-properties-and-functional-applications/chitin-nanofibers-with-a-uniform-width-of-10-to-20-nm-and-their-transparent-nanocomposite-films

INTECH
open science | open minds

InTech Europe
University Campus STeP Ri
Slavka Krautzeka 83/A
51000 Rijeka, Croatia
Phone: +385 (51) 770 447
Fax: +385 (51) 686 166
www.intechopen.com

InTech China
Unit 405, Office Block, Hotel Equatorial Shanghai
No.65, Yan An Road (West), Shanghai, 200040, China
中国上海市延安西路65号上海国际贵都大饭店办公楼405单元
Phone: +86-21-62489820
Fax: +86-21-62489821

IntechOpen